HHS Public Access

Author manuscript

Cell Host Microbe. Author manuscript; available in PMC 2017 October 12.

Published in final edited form as:

Cell Host Microbe. 2016 October 12; 20(4): 482–492. doi:10.1016/j.chom.2016.08.013.

Inflammation-induced adhesin-receptor interaction provides a fitness advantage to uropathogenic *E. coli* during chronic infection

Matt S. Conover[1,#], **Ségolène Ruer**[2,3,#], **Joemar Taganna**[2,3], **Vasilios Kalas**[1], **Henri De Greve**[2,3], **Jerome S. Pinkner**[1], **Karen W. Dodson**[1], **Han Remaut**[*,2,3], and **Scott J. Hultgren**[1,*]

[1]Department of Molecular Microbiology and Center for Women's Infectious Disease Research, Washington University School of Medicine, St. Louis, Missouri, USA

[2]Structural and Molecular Microbiology, Structural Biology Research Center, VIB, Pleinlaan 2, 1050 Brussels, Belgium

[3]Structural Biology Brussels, Vrije Universiteit Brussel, Pleinlaan 2, 1050 Brussels, Belgium

SUMMARY

Uropathogenic *E. coli* (UPEC) is the dominant cause of urinary tract infections, clinically described as cystitis. UPEC express CUP pili, which are extracellular fibers tipped with adhesins that bind mucosal surfaces of the urinary tract. Here we identify the role of the F9/Yde/Fml pilus for UPEC persistence in the inflamed urothelium. The Fml adhesin FmlH binds galactose β1-3 N-acetylgalactosamine found in core-1 and -2 O-glycans. Deletion of *fmlH* had no effect on UPEC virulence in an acute mouse model of cystitis. However, FmlH provided a fitness advantage during chronic cystitis, which is manifested as persistent bacteriuria, high bladder bacterial burdens and chronic inflammation. *In situ* binding confirmed that FmlH bound avidly to the inflamed, but not the naïve bladder. In accordance with its pathogenic profile, vaccination with FmlH significantly protected mice from chronic cystitis. Thus, UPEC employ separate CUP pili to adapt to the rapidly changing niche during bladder infection.

eTOC BLURB

[*]Address correspondence to, Lead Contact: Scott J. Hultgren, hultgren@wusm.wustl.edu, Phone: 314-362-7059, Fax: 314-362-3203.
[*]Address correspondence to: Han Remaut, han.remaut@vib-vub.be, Phone: +32-2-6291923, Fax: +32-2-6291963.
[*]co-corresponding authors
[#]Authors contributed equally

SUPPLEMENTAL INFORMATION

Supplemental Information includes Extended Experimental Procedures, six figures and four tables and can be found with this article online at xxx.

AUTHOR CONTRIBUTIONS

Conceptualization, H.R. and S.J.H.; Methodology, M.S.C, S.R., H.D.G., J.S.P., H.R. and S.J.H.; Investigation, M.S.C, S.R., J.T., J.S.P., V.K. and H.R.; Writing – Original Draft, M.S.C., S.R., K.W.D., H.R. and S.J.H.; Writing – Review & Editing, M.S.C., K.W.D., H.R. and S.J.H.; Funding Acquisition, H.R. and S.J.H.; Resources, M.S.C., S.R., J.T. and J.S.P.; Supervision, H.R. and S.J.H

Uropathogenic *Escherichia coli* (UPEC) express extracellular, adhesion-tipped, fibers that bind mucosal surfaces of the urinary tract. Conover et al. show that urothelial glycome remodeling during ongoing UPEC bladder infection induces the emergence of an F9 pilus receptor, which enables F9 pilus-mediated adherence, late stage colonization and chronic UTI.

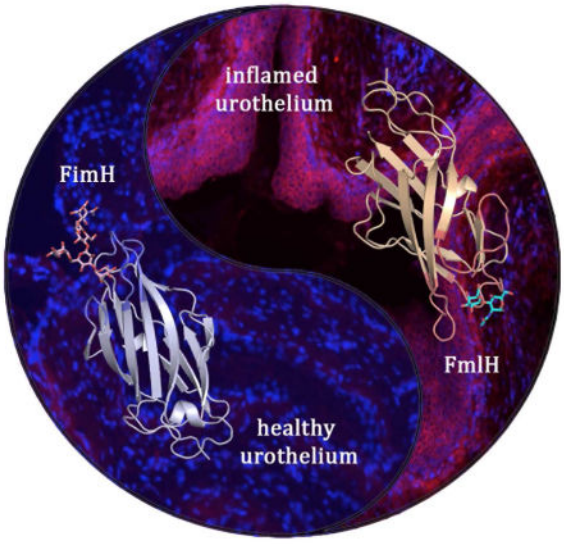

INTRODUCTION

Urinary tract infections (UTI) are one of the most common bacterial infections with 50% of women experiencing a UTI in their lifetime (Ikaheimo et al., 1996). Additionally, an initial acute infection has a 25–40% chance of a recurrent UTI (rUTI) within six months, even with appropriate antibiotic treatment (Czaja et al., 2009; Foxman et al., 2000; Stamm et al., 1991). Further confounding this problem, UPEC, which cause ~80% of such infections, are becoming increasingly antibiotic resistant (Boucher et al., 2009; Chen et al., 2012; Stamm, 2002). Multidrug resistant UPEC increase the risk of UTIs progressing to life-threatening septicemia (Wagenlehner et al., 2015). Thus, there is a pressing need to better understand UPEC pathogenesis in order to inform treatment strategies and therapeutic development.

UPEC, like other gram-negative pathogens including *Klebsiella, Pseudomonas, Haemophilus, Salmonella* and *Yersiniae* utilize chaperone usher pathway (CUP) pili to mediate attachment to both biotic and abiotic surfaces (Nuccio and Baumler, 2007). These extracellular fibers mediate attachment through specific stereochemical interactions with target ligands, most often glycans (Lillington et al., 2014). UPEC encode multiple types of adhesive CUP pili. A recent analysis of available *Escherichia* sequences identified at 38 distinct CUP pilus types based on usher phylogeny (Wurpel et al., 2013). Single *Escherichia* genomes have as many as 16 distinct CUP operons, many encoding two-domain adhesins that likely mediate colonization of a particular host and/or environmental habitat. For example, type 1 pili are critical for bladder colonization in cystitis, while P and S pili function in pyelonephritis and meningitis, respectively (Hultgren et al., 1985; Leffler and Svanborg-Eden, 1980; Saukkonen et al., 1988).

UPEC utilize type 1 pili, and their tip adhesin FimH, to bind the urothelium through interactions with mannosylated uroplakins and α-1/β-3 integrins (Eto et al., 2007; Wu et al., 1996). These FimH-mediated interactions facilitate bacterial colonization and invasion of terminally differentiated superficial umbrella cells (Mulvey et al., 1998; Mulvey et al., 2001). After invasion, UPEC can be expulsed through a TRPML3 dependent mechanism or escape into the cytoplasm where a single bacterium can rapidly divide to form an intracellular bacterial community (IBC), which upon maturation, can contain ~$10^{4–5}$ bacteria (Anderson et al., 2003; Miao et al., 2015; Schwartz et al., 2011). IBCs are transient and upon maturation, UPEC can filament and flux out of these cells to initiate subsequent rounds of IBC formation (Justice et al., 2006). These distinct acute stages of UPEC infection that were first seen in mice are also observed in humans with UTI (Rosen et al., 2007) and has been correlated with increased risk of children developing a rUTI (Robino et al., 2013).

Acute infection can self-resolve or develop into a chronic cystitis characterized by: i) persistent, high titer bacteriuria (>10^4 colony forming units (CFU)/ml); ii) high titer bacterial bladder burdens at sacrifice >4 weeks post-infection (wpi); iii) chronic inflammation and urothelial necrosis; iv) lymphonodular hyperplasia in the bladder submucosa and; v) urothelial hyperplasia with a lack of uroplakin expression, which is a marker for terminal differentiation in superficial facet cells (Hannan et al., 2010). Similar histological findings have been observed in humans suffering persistent bacteriuria and rUTI (Hansson et al., 1990; Schlager et al., 2011).

The function of FimH in pathogenesis has been well studied, however, *E. coli* carry 12 CUP operons on average per genome, inferring a depth and diversity of function (Wurpel et al., 2013). Sequence comparison has revealed that the Fml/F9/Yde pilus is the closest related pilus to type 1 pili (Wurpel et al., 2013). Given the close relationship between these pili and the pathogenic role of FimH in UTI, we hypothesized that Fml pili may play a role in pathogenesis. In this study we report the structure of the Fml tip-associated adhesin, FmlH and its specificity for binding Gal(β1-3)GalNac epitopes. We demonstrate that FmlH functions in UPEC pathogenesis by providing a fitness advantage during chronic cystitis but not in acute cystitis. Consistent with these findings, FmlH binds to inflamed bladder tissue of chronically infected mice, but not to naïve bladder tissue. Further, we elucidated that chronic cystitis alters the glycan/galactose profile of mouse bladders, and UPEC expression of *fml* is upregulated in chronically infected bladders. We showed clinical relevance of these findings by demonstrating that FmlH binds human urothelial cells and uromodulin isolated from human urine. In addition, analysis of published data showed higher expression of FmlH in urines directly isolated from UTI patients compared to expression during *in vitro* growth in media or normal urine, suggesting host-specific Fml induction (Subashchandrabose et al., 2014). On the basis of these findings, we developed an FmlH vaccine, and showed significantly decreased bacterial colonization after the initial acute stages of infection with potential therapeutic implications.

RESULTS

Role of F9 pili in UTI pathogenesis

Phylogenetic analysis of *E. coli* CUP operons shows type 1, S and F1C pili form a monophyletic cluster with F9 pili (*fml; E. coli* CFT073 *c1931-c1936*), suggesting they originated through gene duplication from a common ancestral CUP operon (Figure S1A,B) (Wurpel et al., 2013). Additionally, the presence of complete *fml* pilus operons was found to be enriched in UPEC isolates Figure S1A, (Wurpel et al., 2014) and transcriptomic data indicate that F9 pili are expressed in the urine of women with UTI (Subashchandrabose et al., 2014; Welch et al., 2002b). Thus, we investigated the function of F9 pili during UTI in well-established C3H/HeN mouse models of UTI (Hannan et al., 2010; Hopkins et al., 1996; Hopkins et al., 1998; Schwartz et al., 2011).

We performed competitive infections between the prototypical UPEC strain CFT073 and an isogenic strain (CFT073*ΔfmlH)* with a deletion of *fmlH,* which encodes the predicted adhesive subunit FmlH (Figure S1B) each carrying different antibiotic markers (Welch et al., 2002a). Bacteriuria was monitored over a 28-day time course. One day post-infection (dpi) no difference in urine titers of these strains was observed. However, a competitive defect of CFT073*ΔfmlH* was evident in bacteriuria counts 3 dpi but was most clearly observed 10–28 dpi (Figure 1A and S1D). At 28 dpi, CFT073*ΔfmlH* was outcompeted by CFT073 by ~1000 and ~100 fold in the bladder and kidneys, respectively, as assessed by CFU determination of harvested tissue homogenates (Figure 1B and S1D). *In vitro* cultures showed no growth difference in CFT073 and CFT073*ΔfmlH* (Figure S1C), indicating the competitive defect of the mutant was specific to the *in vivo* context. Additionally, CFT073*ΔfmlH:fmlH,* a strain with *fmlH* reintegrated into the original deletion site, showed no significant competitive difference compared to CFT073 (Figure 1C and S1E). In single infections, CFT073*ΔfmlH* also exhibited attenuated virulence compared to CFT073 as observed by infection outcome. Only 17% of C3H/HeN mice infected with $1x10^8$ cfu of CFT073*ΔfmlH* developed chronic infection, characterized by persistent bacteriuria and bladder inflammation (Figure S2), compared to 38% infected with CFT073 (Figure 1D). Thus, both single and competitive colonization profiles suggest that FmlH engages in critical interactions for the establishment and/or maintenance of chronic cystitis.

Identification of the FmlH receptor

To confirm FmlH is the F9 adhesin and to determine its glycan specificity, FmlH's predicted N-terminal adhesin domain ($FmlH^{AD}$, residues 1-158) was cloned, purified and binding profiles to the core H mammalian glycan array (Consortium for Functional Glycomics (CFG)). $FmlH^{AD}$ bound to N-acetylgalactosamine (GalNAc), Galβ1-3GalNAc as well as GlcNAc β1-6(Galβ1-3)GalNAc, the latter two representing the basal structures of Core 1 (commonly called Thomsen-Friedenreich or TF antigen) and Core 2 O-glycans, respectively (Figure 2A, Table S1). The array data indicated that additional modification in the GlcNAcβ1-6 branch of the Core 2 glycans is accepted, but suggested that the short Galβ1-3GalNAc – branch of the glycans needs to be unmodified and forms the common epitope of FmlH receptors (Table S1). Core 1 and 2 O-glycans are abundant in secreted mucosal proteins such as mucins, where they are frequently capped by terminal sialic acid

(Table S1). We therefore performed *in vitro* enzyme linked immunosorbent assays (ELISA) using a model O-glycosylated mucosal protein, bovine submaxillary mucin (BSM), with or without sialidase pre-treatment (Tsuji and Osawa, 1986). FmlH^{AD} displayed robust binding upon enzymatic removal of terminal sialic acid residues to BSM, but showed little to no affinity to untreated BSM (Figure 2C). As controls, Peanut agglutinin (PNA) and *Helix pomatia* agglutinin (HPA), which recognize exposed Galβ1-3GalNAc or α-GalNAc respectively (Loris et al., 1994; Sanchez et al., 2006) displayed similar BSM binding patterns as FmlH with removal of terminal sialic acid enhancing binding (Figure S3B, C). In addition, in whole cell ELISA, CFT073 adhered to sialidase treated BSM and CFT073*ΔfmlH* showed decreased binding, which was restored by plasmid-based *fmllH* complementation, (Figure 2D).

To obtain relative binding affinities of FmlH for specific ligands we used Surface Plasmon Resonance (SPR). FmlH^{AD} bound TF antigen and Core2 glycans with similar equilibrium dissociation constants (Kds) of 17.4μM and 12.2μM respectively, thus showing the Core2 branch glycan (GlcNAcβ1-6) can be accommodated but does not add binding affinity (Figure 2B). Solution binding studies for the component monosaccharides of the Galβ1-3GalNAc epitope showed binding affinities of 625 and 961 μM for D-Gal and Tn (αGalNAc), respectively (Figure S3A). In accordance with the SPR data, the lactosyl disaccharide that is added in the Core2 branch of the glycans did not show a detectable binding interaction with the adhesin (Figure S3A). Thus, we propose that FmlH preferentially binds Galβ1-3GalNAc and terminal α-GalNAc, both of which are components of core-1 and 2 O glycans.

Structure-function correlates of FmlH

To gain insight into the molecular determinants of FmlH receptor interactions we determined the X-ray structures of FmlH^{AD} in apo form and in complex with Galβ1-3GalNAc. Apo FmlH^{AD} adopts a 12-stranded immunoglobulin-like β-sandwich topology closely resembling the FimH lectin domain structure (Choudhury et al., 1999) with a root mean squared deviation (RMSD) of 1.3 Å for 147 matching Cα residues (Figure 3A). In FimH, three loops connecting β-strands A1 and A2 (Loop 1, residues 6-15), B2 and C1 (Loop 2, residues 44-53) and F and G (Loop 3, residues 132-142) form a confined binding pocket that binds terminal D-mannose residues (Figure 3A, S4B). These three loops coincide with the regions with highest sequence and structural divergence between FimH and FmlH (Figure 3A, S4A). Co-crystallization of FmlH^{AD} with Galβ1-3GalNAc reveals the FmlH L1–L3 loops constitute a TF antigen-binding site, equivalent to the FimH D-mannose binding pocket (Figure 3B). Similar to FimH, the FmlH-TF interaction is dominated by an extensive H-bond network with the terminal, non-reducing residue of the glycan epitope (Figure 3B, S4B). The terminal Gal residue makes a stacking interaction with Y46 and eight H-bond interactions with the FmlH binding pocket, compared to a single H-bond between Y46 and the β1-3GalNAc N-acetyl (Figure 3B, D). Mannose and galactose differ in configuration of the C2 and C4 stereogenic centers. Superimposition of the FimH oligomannose-3 (Wellens et al., 2008) and FmlH Galβ1-3GalNAc complexes shows residues at positions 132 and 134 (Q and N for FimH vs. K and A for FmlH, respectively) play a prominent role in determining the monosaccharide binding specificities of the respective binding sites (Figure

3D). The FmlH K132 - C3 hydroxyl interaction tilts the monosaccharide upwards and allows K132 to additionally bind Gal's axial C4 hydroxyl. The upwards tilt also projects the equatorial C2 hydroxyl within H-bond distance of N140. In FimH, the C3 – Q133 H-bond pulls the mannose (Man) residue in a downward tilt, allowing Man's axial C2 hydroxyl to H-bond with the F1 amine. Man's equatorial C4 hydroxyl is H-bonded by the N135 (Figure 3D). The binding topology of the Galβ1-3GalNAc – FmlH interaction explains the requirement for unmodified C3, C4 and C6 positions in the terminal Gal residues, and the requirement for sialic acid uncapping of Core 1 and 2 O-glycans for F9-mediated adherence (Figure 2). Superimposition of the Galβ1-3GalNAc – FmlH structure with an energy-minimized Core 2 glycan shows that the GlcNAcβ1-6 residue in the Core 2 branch localizes above the FmlH molecular surface where it can accept further modifications (Figure S4D), in agreement with the binding profiles observed by glycan array (Table S1). Based on the very similar binding affinities for Core 2 and Core 1 glycans (Figure 2B) and the modeled binding position of the Core 2 GlcNAcβ1-6, no additional H-bond or stacking interactions are expected on top of the interaction with the Galβ1-3GalNAc epitope (Figure S4D).

For independent confirmation of the observed binding interactions, we examined the effects of selected mutations in the FmlH pocket residues on F9-mediated adherence. D53 was mutated to either a glutamic acid (D53E) or lysine (D53K) to alter charge and/or bulk inside the galactose-binding pocket. Additionally, K132 was changed to the FimH-like glutamine (K132Q), thus altering positioning and H-bonding capacity of Gal in the FmlH binding pocket. We found that D53E, D53K, and K132Q all dramatically decreased $FmlH^{AD}$ affinity for sialidase treated BSM to background levels (Figure 3C).

Binding of FmlH to human bladder cells and uromodulin

We next assessed the presence of FmlH receptor in immortalized urothelial cells by assessing binding to 5637 and T24 human bladder cells. Since bladder biopsies during clinical UTI are contraindicated due to risk of sepsis, bladder tissue from UTI patients is unavailable. The 5637 cell line originates from a male grade II bladder carcinoma and the T24 cells originate from a female transitional carcinoma (Bubenik et al., 1973; Fogh et al., 1977). When these cells are grown in culture they resemble transitional urothelial cells since they do not differentiate into superficial facet cells, are rapidly dividing and do not express uroplakin on the cell surface (Eto et al., 2007). We found that $FmlH^{AD}$, but not K132Q $FmlH^{AD}$, bound to both of these cell lines, demonstrating that cells of an urothelial lineage can support FmlH binding (Figures 4A and S5). Additionally, we tested for the presence of FmlH receptors on secreted proteins in the UT. Far-western analysis of concentrated total human urine protein revealed binding of $FmlH^{AD}$, but not $FmlH^{AD}$ K132Q, to a band of approximately ~85 KDa, identified as uromodulin by N-terminal sequencing (Figure 4B). Uromodulin is heavily O-glycosylated and contains possible FmlH binding epitopes including Gal(β1-3)GalNac (Chia-Yean Hong, 2013). Human uromodulin (Tamm-Horsfall) is abundantly secreted by the kidneys into the urine (Tamm and Horsfall, 1950). This protein functions as an inhibitor of calcium crystallization and has been proposed to be part of an innate immune defense mechanism against UPEC by presenting soluble decoy receptors for the FimH adhesin (Bates et al., 2004; Pak et al., 2001). In an ELISA based technique both FimH and FmlH displayed a concentration-dependent binding to urine protein concentrates

enriched for uromodulin; with FimH binding being 10 fold greater, possibly reflecting FimH nanomolar versus FmlH's micromolar dissociation constants for their preferred epitopes (Figure 4C, D). FmlH^{AD} K132Q and FimH Q133K, displayed little to no affinity in this assay (Figure 4C, D). Together these data suggest that the innate immune defense protein uromodulin may have in part evolved as a host defense against tissue binding via numerous UPEC adhesins.

FmlH-mediated host-pathogen interactions in the urinary tract

Many aspects of host-pathogen interactions, as well as disease outcomes and host responses observed in human UTIs have been successfully replicated in the mouse model UTI (Garofalo et al., 2007; Hannan et al., 2014; Rosen et al., 2007). Since *fmlH* deletion decreased virulence during chronic infection (Figure 1), we examined the spatio-temporal distribution of the FmlH receptors in the mouse UT. Microscopic analysis of an FmlH^{AD}-mCherry fusion protein (FmlH^{ADmC}) was used to probe binding to inflamed and naïve bladder and kidney tissue sections *in situ*. Kidney tissue supported strong FmlH^{ADmC} binding in both naïve and chronically infected mice (Figure 5A and S6A). This staining appeared to correlate with staining of the distal convoluted tubules (Figure 5A and S6B). In contrast, FmlH^{ADmC} displayed little to no affinity for naïve bladder tissue (Figure 5F), but bound avidly to tissue sections from infected (inflamed) bladders (Figure 5I). FmlH bound throughout the transitional urothelial cell layer, which due to the exfoliation of the superficial cells during acute cystitis, is exposed on the luminal surface of the bladder. Thus, our data argue for a constitutive exposure of the FmlH receptor in mouse kidney, but suggest that the FmlH receptor only becomes exposed during the inflammatory response to infection that leads to a shift or modification of the glycan expression profile.

During chronic/recurrent UTI the bladder becomes markedly inflamed and hyperplastic, denoting a dramatically altered tissue compared to the naïve bladder, as described and reviewed in (Hannan et al., 2010; Hannan et al., 2014; Hannan et al., 2012; O'Brien et al., 2015). Further, proteomic studies showed that chronic cystitis results in urothelial remodeling that persists even after antibiotic therapy and into convalescence (Hannan et al., 2014). In the kidney, PNA appeared to co-localize with FmlH^{ADmC} binding (Figure 5E) and recognition of both was abolished by prior O-glycosidase treatment (Figure 5C–D), suggesting that in the kidney FmlH binds O-linked polysaccharides that contain uncapped Galβ1-3GalNAc. However, in the bladder, PNA staining was not observed in either chronic or naïve bladder tissue (Figure 5G,J). Prior sialidase treatment did not reveal significant urothelial PNA or FmlH^{ADmC} staining in naïve urothelium (Figure S6C,E,F), indicating that the lack of binding was not due to the capping of O-glycans by terminal sialic acid. Additionally, O-glycosidase treatment of chronic bladder tissue did not prevent FmlH^{ADmC} staining (Figure S6D), suggesting FmlH is not binding mature O-glycans in the bladder. Our glycan array shows that besides Galβ1-3GalNAc, FmlH^{AD} can also bind terminal α-N-acetylgalactosamine (Figure 2). Staining with HPA as a reporter for terminal α-N-acetylgalactosamine demonstrated affinity to the transitional epithelial cells in chronic bladder sections, as well as the basal membrane in both naïve and chronic bladders (Figure 5H,K). Sialidase treatment did not influence HPA staining on either chronic or naïve bladder sections (Figure S6G,H). While FmlH^{ADmC} did not bind the basal membrane in the bladder

(Figure 5F), its inflammation-induced binding in the transitional cell layer during chronic cystitis is very similar to that seen for HPA (Figure 5K). Treatment of chronic bladder sections with alpha-N-acetyl-galactosaminidase decreased $FmlH^{ADmC}$ and HPA binding, especially in the transitional cell layer (Figure 5L,N). Further, co-staining of chronic bladder with HPA and $FmlH^{ADmC}$ resulted in an overlap of signal (Figure 5M) suggesting binding of a similar ligand or structure. Thus our staining analyses suggest that FmlH, at least in part, recognizes αGalNAc that becomes exposed in the bladder during an inflammatory response to infection.

FmlH and FmlH receptor expression during chronic cystitis

The dramatic increase in the affinity of FmlH for the inflamed bladder epithelium suggests that the glycan, and more specifically the terminal Gal and GalNAc profiles of the urothelium change during chronic cystitis. Notably, Ser-/Thr-linked αGalNAc (Tn antigen) forms the precursor of O-glycan synthesis. Tn antigen is rare on healthy tissues, but changes in tissue homeostasis, including inflammation and malignant transformation, can result in a stalled O-glycan maturation and Tn antigen accumulation (Ju et al., 2011). We, thus, performed qPCR on naïve and chronic bladder samples and found that *c1galt*, *galnt3*, *b3gnt3*, *b4galnt1*, *ggta1* and *galnt4* were all upregulated during chronic cystitis (Figure 6A). C1GALT, and the polypeptide GalNAc transferases GALNT4 and GALNT3, catalyze the synthesis of the TF and the Tn antigens, respectively. Further, FmlH has been shown to be upregulated in *E. coli* found in the urine of women with UTI (Subashchandrabose et al., 2014). Thus, we performed qPCR on tissue-associated CFT073 harvested from chronically infected bladders 28 dpi. We observed that expression of *fmlA*, the major F9 subunit, was increased approximately 6 fold during chronic cystitis when compared to the inoculum (Figure 6B). While the expression pattern of *fimI*, a representative gene of the *fim* locus, revealed no further induction of type 1 pili relative to the inoculum (Figure 6B). Thus, it appears that as the host bladder is being remodeled by chronic infection, UPEC is adapting to this environment by upregulating the FmlH adhesin whose receptors are being revealed during this process.

FmlH vaccination

We hypothesized that vaccination with FmlH would protect against chronic/recurrent cystitis when the bladder becomes inflamed, similar to the protection against acute UTI seen with FimH vaccination (Firon et al., 1987; Langermann and Ballou, 2001; Langermann et al., 2000). To test this we vaccinated mice with 30μg of $FmlH^{AD}$ in Freund's complete adjuvant for 4 weeks before boosting with a second 30μg dose in Freund's incomplete adjuvant. Mice were challenged with CFT073 4 weeks after boost and bacterial titers were assessed 1, 2 and 3 dpi. One dpi there was no significant difference in bacterial load between the mock vaccinated animals or the ones vaccinated with $FmlH^{AD}$ (Figure 7). However, by 2 and 3 dpi a significant decrease in UPEC colonization was seen in mice that received the $FmlH^{AD}$ vaccine (Figure 7). While we did not measure inflammatory readouts at these time points, the bacterial load is significantly diminished compared to mock vaccination. Thus, vaccination with $FmlH^{AD}$ protected against UPEC colonization during the chronic stages of infection when FmlH plays a significant role in host-pathogen interactions.

DISCUSSION

Progression from acute to chronic cystitis is accompanied by a loss of superficial facet cells through exfoliation; an influx of polymorphonuclear leukocytes, mononuclear lymphocytes and $CD45^+$ cells and; a hyperplastic transitional epithelial cell layer which is poorly differentiated, containing few terminally differentiated umbrella cells accounting for the lack of uroplakin III staining, a marker of superficial cell differentiation (Hannan et al., 2010; Hannan et al., 2014). Markers of inflammation are also present in the lamina propria where lymphoid-like $CD45^+$ follicle-like aggregates are histologically visible. This is a much altered environment compared to the naive bladder first encountered by UPEC during acute cystitis. Herein we present evidence of UPEC adaptation to the changing UTI environment by expressing a Gal/GalNAc recognizing adhesin at the same time as alteration to the host glycan expression are occurring in the inflamed bladder habitat. We discovered that FmlH is expressed during chronic inflammation. Others have shown that FmlH is expressed during human UTI (Subashchandrabose et al., 2014). Our structural and binding analysis revealed that FmlH binds Gal(β1-3)GalNAc as its primary ligand, but also displays affinity to its precursor, αGalNAc. Our histological studies suggest that FmlH binds, at least in part, to αGalNAc exposed during chronic cystitis. While the proteinaceous ligand for FmlH during chronic cystitis is unknown, it is likely connected with a Tlr4 inflammatory process since Tlr4 is necessary for CFT073, and other stains, to cause chronic cystitis in the C3H background (our unpublished results and (Hannan et al., 2010)). Alternately, in the kidney, FmlH appears to bind constitutively exposed Gal(β1-3)GalNAc, often found in core 1 and 2 O-glycans, possibly reflecting the kidney epithelia's secretion of glycoproteins like Muc1 and uromodulin.

Glycan alteration in response to disease has been well documented in the bladder. Previous reports have shown diabetes alters the expression of several sugar moieties in the bladder including mannose, galactose and N-acetlyglucosamine (Ozer et al., 2015). These changes likely provide receptors that can be recognized by adhesins such as FimH and FmlH. In fact, previous reports have shown that FimH displays increased affinity to the diabetic bladder compared to non-diabetic controls (Geerlings et al., 2002; Ozer et al., 2015). Further, our results (Figure 6) are in agreement with the glycan remodeling seen in a recent study of the mouse bladder transcriptome during chronic cystitis, which revealed the alteration of many glycosyl transferases including 20 involved in modifying the galactose epitopes such as C1GALT, GALNT4, B3GNT3 and GALNT3 that can make or modify Gal(β1-3)GalNAc (Schwartz et al., 2015). Finally, studies looking at specific lectin binding to naïve and inflamed rat bladders chronically exposed to UPEC showed a very similar phenotype to what we observe in mice with increased expression of Gal and GalNAc epitopes (Nakagawa et al., 1996).

Bladder remodeling associated with UTI, including superficial cell exfoliation, chronic inflammation and urothelial hyperplasia, has been well documented in mice (Hannan et al., 2014). Similar phenotypes are associated with human UTI where exfoliation, IBCs and inflammation routinely occur with UPEC infection (Czaja et al., 2009; Rosen et al., 2007). Additionally, biomarkers associated with myeloid cell development and chemotaxis have been shown to be elevated in individuals who are prone to rUTI, suggesting an altered

bladder environment in this population (Hannan et al., 2014). While these similarities to the mouse model and data presented herein infer a role for FmlH in human disease, further studies are needed to determine whether FmlH plays a similar role in binding the inflamed bladder in humans as it does in mice. Notably, FmlH has also been shown to be upregulated between 4 and 64 fold in bacteria recovered in each of 5 human UTI urine samples/isolates compared to growth in standard LB conditions (Subashchandrabose et al., 2014). Interestingly, this upregulation was most dramatic in urines taken directly from human UTI and tempered when grown *in vitro* in normal human urine suggesting that the host-specific induction we see in our mouse model may also take place within the inflamed human bladder during clinical UTI.

It has been well documented that antibiotic resistance is increasing among UPEC isolates, thus evoking a need for alternate therapeutics. Therapeutic/preventitive strategies targeting bacterial adhesion have shown promise including small molecules called mannosides that bind to the FimH binding pocket with 10^6 greater potency than mannose and have been shown to be orally bioavailable and potent in treating UTI in a mouse model (Cusumano et al., 2011a; Han et al., 2012). Further, a FimCH vaccine has been developed that elicits protection against UTI in mouse and monkey models and currently is in phase 1 clinical trials (Cusumano et al., 2011b; Langermann and Ballou, 2001; Langermann et al., 2000) (Gary Eldridge, personal communication). We show that vaccination with purified FmlH lectin domain is sufficient to decrease UPEC burden as early as 2dpi. This data implies that inhibition of FmlH reduces UPEC colonization making it, or an FmlH/FimH combination, another possible target for improved vaccination techniques or galactose analogue inhibition similar to mannosides with FimH.

EXPERIMENTAL PROCEDURES

Strains and Plasmids

The pyelonephritis isolate CFT073 was utilized as the wild type isolate for these studies. CFT073Δ*fmlH* was constructed using the λ Red Recombinase system to insert a kanamycin cassette in place of *fmlH* (Table S3). Complementation of CFT073Δ*fmlH* was accomplished by cloning the *fmlH* gene into pTRC99a using Kpn1 and Xba1 sites (Table S3). CFT073*ΔfmlH:fmlH* was constructed by homologous recombination to reintegrate *fmlH* into the *ΔfmlH* strain using homologous recombination with a modified λ Red Recombinase system (Khetrapal et al., 2015).

Mouse experiments

UPEC strains were grown statically in LB at 37°C overnight and then subcultured 1:1,000 into 10 ml of fresh LB for a second static outgrowth at 37°C for 18 to 24 h. From these cultures, $1x10^8$ bacteria suspended in PBS were inoculated into lightly anesthetized C3H/HeN mice transurethrally in a 50μl injection. For competitive infections, strains were inoculated with equal CFU of CFT073, *ΔfmlH* or *ΔfmlH:fmlH* carrying either chloramphenicol or kanamycin resistance markers. Infections proceeded for 28 days with urines collected at indicated time points before sacrifice under anesthesia, and the bladders and kidneys were removed and homogenized in sterile PBS. Homogenates were plated for

bacterial enumeration. Competitive infections were initiated by mixing $1x10^8$ bacteria from each indicated strain in the inoculum. These strains carried different antibiotic markers, which allowed for the tracking of bacterial titers of the individual strains throughout the time course. For competitive infections, sterile urines were processed as the limit of detection for determining the competitive index. As previously published, most C3H/HeN mice (~60%) are capable of resolving an acute UTI (Hannan et al., 2010). Mice that developed persistent bacteriuria ($>10^4$ cfu/ml) were considered chronically infected, as has been shown previously to be predictive of chronic cystitis (Hannan et al., 2010). All animal studies using mice were approved by the Animal Studies Committee of Washington University (Animal Protocol Number 20120216).

FmlH constructs and purification

$FmlH^{AD}$ corresponds to the first 158 amino acids of mature FmlH (CFT073). The corresponding gene sequence was cloned into expression vector pDEST14 with its natural leader and a 6 His tag and stop codon incorporated at the 3′ end. $FmlH^{ADmC}$ corresponds to $FmlH^{AD}$ with mCherry fused between the $FmlH^{AD}$ C-teminus and the 6 His tag. All proteins were expressed in the periplasm of *E. coli* C43(DE3). Periplasmic extracts were dialyzed against 1xPBS, bound to a Cobalt (Goldbio) column and eluted with 1xPBS and 200mM imidazole. Pooled fractions containing $FmlH^{AD}$ were dialyzed against 20mM Tris pH 8.4 and applied to a Source 15Q and eluted at 100mM NaCl.

Crystallization and structure determination

$FmlH^{AD}$ (8mg mL^{-1}) was crystallized using sitting drop vapor diffusion against a solution containing 0.1M Citrate pH2, 1M Ammonium sulfate. $FmlH^{AD}$ crystals were flashed cooled to 100K in 0.1M Citrate pH2, 1M Ammonium sulfate and 30% glycerol. For co-crystallization, His-tagged $FmlH^{AD}$ (24mg ml^{-1}) was incubated with 1mM Thomsen-Friedenreich sugar (TF: Galβ1-3GalNAc) (Lectinity, Russia). Data for $FmlH^{AD}$ apo (1.75 Å) and $FmlH^{AD}$-TF (2.2 Å) were collected at beamline i04 (Diamond Light Source, Didcot, UK). Data were indexed and processed with XDS and XSCALE (Kabsch, 2010), phased by molecular replacement [Phaser (Collaborative Computational Project, 1994)] using coordinates of FimH (PDB:2VCO) and refined using Refmac5.5 (The CCP4 suite: programs for protein crystallography., 1994). Data and refinement statistics in Table S2.

Vaccination

$FmlH^{AD}$ was emulsified in Freud's complete adjuvant at a final concentration of 300μg/ml. C3H/HeN mice were injected subcutaneously with 100μl of this emulsion for an effective dose of 30μg per animal. Mock-vaccinated animals received PBS emulsified in the same concentrations of the adjuvant. Four weeks after initial injection, a boost dose of 30μg of FmlH or PBS emulsified in Freud's incomplete adjuvant was given to each vaccinated animal and control animals, respectively. Anti-FmlH titers were monitored throughout the time course to assess antibody response. Mice were challenged with $2x10^8$ CFU of CFT073 inoculated transurethrally 4 weeks after boost. Animals were sacrificed 1, 2 and 3 dpi and the bacterial titers were assessed in the bladder and kidneys. These time points were chosen since naïve aged mice are relatively resistant to chronic cystitis.

Supplementary Material

Refer to Web version on PubMed Central for supplementary material.

Acknowledgments

We would like to acknowledge Nathaniel Gualberto for his cloning expertise and Tam Mignot for the gift of the pSWU19 plasmid. We would also like to thank Danielle Liu and Mike Hibbing for their assistance with mouse experiments. We acknowledge the kind support of beamline staff at PROXIMA1 - SOLEIL and i04 - Diamond Light Source, as well as the participation of the Protein–Glycan Interaction Resource of the CFG. This work was funded through SJH- P50 DK064540, R01 DK051406, and R01 AI048689; MC- F32 DK101171-02; HR-G030411N (FWO) and UABR/09/005 (Hercules foundation). Scott Hultgren has a financial ownership in Fimbrion and may financially benefit if the company is successful in marketing the mannosides related to this research and may receive royalty income based on the FimH vaccine technology that he developed which was licensed by Washington University to Sequoia Sciences.

References

Anderson GG, Palermo JJ, Schilling JD, Roth R, Heuser J, Hultgren SJ. Intracellular bacterial biofilm-like pods in urinary tract infections. Science. 2003; 301:105–107. [PubMed: 12843396]

Bates JM, Raffi HM, Prasadan K, Mascarenhas R, Laszik Z, Maeda N, Hultgren SJ, Kumar S. Tamm-Horsfall protein knockout mice are more prone to urinary tract infection: rapid communication. Kidney Int. 2004; 65:791–797. [PubMed: 14871399]

Boucher HW, Talbot GH, Bradley JS, Edwards JE, Gilbert D, Rice LB, Scheld M, Spellberg B, Bartlett J. Bad bugs, no drugs: no ESKAPE! An update from the Infectious Diseases Society of America. Clin Infect Dis. 2009; 48:1–12. [PubMed: 19035777]

Bubenik J, Baresova M, Viklicky V, Jakoubkova J, Sainerova H, Donner J. Established cell line of urinary bladder carcinoma (T24) containing tumour-specific antigen. International journal of cancer Journal international du cancer. 1973; 11:765–773. [PubMed: 4133950]

Chen YH, Ko WC, Hsueh PR. The role of fluoroquinolones in the management of urinary tract infections in areas with high rates of fluoroquinolone-resistant uropathogens. European journal of clinical microbiology & infectious diseases: official publication of the European Society of Clinical Microbiology. 2012; 31:1699–1704.

Chia-Yean Hong MA, Nyet-Kui Wong. Evaluation of gylcan profiles of Tamm Horsfall glycoprotein and uromodulin. International Journal of Pharmacy and Pharmaceutical Sciences. 2013; 5:385–389.

Choudhury D, Thompson A, Stojanoff V, Langermann S, Pinkner J, Hultgren SJ, Knight SD. X-ray structure of the FimC-FimH chaperone-adhesin complex from uropathogenic Escherichia coli. Science. 1999; 285:1061–1066. [PubMed: 10446051]

Cusumano CK, Pinkner JS, Han Z, Greene SA, Ford BA, Crowley JR, Henderson JP, Janetka JW, Hultgren SJ. Treatment and prevention of urinary tract infection with orally active FimH inhibitors. Science translational medicine. 2011a; 3:109–115.

Cusumano CK, Pinkner JS, Han Z, Greene SE, Ford BA, Crowley JR, Henderson JP, Janetka JW, Hultgren SJ. Treatment and prevention of urinary tract infection with orally active FimH inhibitors. Science translational medicine. 2011b; 3:109ra115.

Czaja CA, Stamm WE, Stapleton AE, Roberts PL, Hawn TR, Scholes D, Samadpour M, Hultgren SJ, Hooton TM. Prospective cohort study of microbial and inflammatory events immediately preceding Escherichia coli recurrent urinary tract infection in women. J Infect Dis. 2009; 200:528–536. [PubMed: 19586416]

Eto DS, Jones TA, Sundsbak JL, Mulvey MA. Integrin-mediated host cell invasion by type 1-piliated uropathogenic Escherichia coli. PLoS Pathog. 2007; 3:e100. [PubMed: 17630833]

Firon N, Ashkenazis S, Mirelman D, Ofek I, Sharon N. Aromatic a-glycosides of mannose are powerful inhibitors of the adherence of type 1 fimbriated *Escherichia coli* to yeast and intestinal cells. Infection and immunity. 1987; 55:472–476. [PubMed: 3542836]

Fogh J, Fogh JM, Orfeo T. One hundred and twenty-seven cultured human tumor cell lines producing tumors in nude mice. Journal of the National Cancer Institute. 1977; 59:221–226. [PubMed: 327080]

Foxman B, Barlow R, D'Arcy H, Gillespie B, Sobel JD. Urinary tract infection: self-reported incidence and associated costs. Ann Epidemiol. 2000; 10:509–515. [PubMed: 11118930]

Garofalo CK, Hooton TM, Martin SM, Stamm WE, Palermo JJ, Gordon JI, Hultgren SJ. Escherichia coli from urine of female patients with urinary tract infections is competent for intracellular bacterial community formation. Infection and immunity. 2007; 75:52–60. [PubMed: 17074856]

Geerlings SE, Meiland R, Hoepelman AI. Pathogenesis of bacteriuria in women with diabetes mellitus. International journal of antimicrobial agents. 2002; 19:539–545. [PubMed: 12135845]

Han Z, Pinkner JS, Ford B, Chorell E, Crowley JM, Cusumano CK, Campbell S, Henderson JP, Hultgren SJ, Janetka JW. Lead optimization studies on FimH antagonists: discovery of potent and orally bioavailable ortho-substituted biphenyl mannosides. Journal of medicinal chemistry. 2012; 55:3945–3959. [PubMed: 22449031]

Hannan TJ, Mysorekar IU, Hung CS, Isaacson-Schmid ML, Hultgren SJ. Early Severe Inflammatory Responses to Uropathogenic E-coli Predispose to Chronic and Recurrent Urinary Tract Infection. PLoS Pathog. 2010:6.

Hannan TJ, Roberts PL, Riehl TE, van der Post S, Binkley JM, Schwartz DJ, Miyoshi H, Mack M, Schwendener RA, Hooton TM, et al. Inhibition of Cyclooxygenase-2 Prevents Chronic and Recurrent Cystitis. Journal of Womens Health. 2014; 23:875–876.

Hannan TJ, Totsika M, Mansfield KJ, Moore KH, Schembri MA, Hultgren SJ. Host-pathogen checkpoints and population bottlenecks in persistent and intracellular uropathogenic Escherichia coli bladder infection. FEMS Microbiol Rev. 2012; 36:616–648. [PubMed: 22404313]

Hansson S, Hanson E, Hjalmas K, Hultengren M, Jodal U, Olling S, Svanborg-Eden C. Follicular cystitis in girls with untreated asymptomatic or covert bacteriuria. J Urol. 1990; 143:330–332. [PubMed: 2405189]

Hopkins W, Gendron-Fitzpatrick A, McCarthy DO, Haine JE, Uehling DT. Lipopolysaccharide-responder and nonresponder C3H mouse strains are equally susceptible to an induced Escherichia coli urinary tract infection. Infection and immunity. 1996; 64:1369–1372. [PubMed: 8606102]

Hopkins WJ, Gendron-Fitzpatrick A, Balish E, Uehling DT. Time course and host responses to Escherichia coli urinary tract infection in genetically distinct mouse strains. Infection and immunity. 1998; 66:2798–2802. [PubMed: 9596750]

Hultgren SJ, Porter TN, Schaeffer AJ, Duncan JL. Role of Type-1 Pili and Effects of Phase Variation on Lower Urinary-Tract Infections Produced by Escherichia-Coli. Infection and immunity. 1985; 50:370–377. [PubMed: 2865209]

Ikaheimo I, Silvennoinen-Kassinen S, Karvonen J, Jarvinen T, Tiilikainen A. Immunogenetic profile of psoriasis vulgaris: association with haplotypes A2,B13,Cw6,DR7,DQA1*0201 and A1,B17,Cw6,DR7,DQA1*0201. Arch Dermatol Res. 1996; 288:63–67. [PubMed: 8932582]

Ju T, Otto VI, Cummings RD. The Tn antigen-structural simplicity and biological complexity. Angew Chem Int Ed Engl. 2011; 50:1770–1791. [PubMed: 21259410]

Justice SS, Hunstad DA, Seed PC, Hultgren SJ. Filamentation by Escherichia coli subverts innate defenses during urinary tract infection. Proc Natl Acad Sci USA. 2006; 103:19884–19889. [PubMed: 17172451]

Khetrapal V, Mehershahi K, Rafee S, Chen S, Lim CL, Chen SL. A set of powerful negative selection systems for unmodified Enterobacteriaceae. Nucleic acids research. 2015; 43:e83. [PubMed: 25800749]

Langermann S, Ballou WR Jr. Vaccination utilizing the FimCH complex as a strategy to prevent Escherichia coli urinary tract infections. J Infect Dis. 2001; 183:S84–86. [PubMed: 11171023]

Langermann S, Mollby R, Burlein JE, Palaszynski SR, Auguste CG, DeFusco A, Strouse R, Schenerman MA, Hultgren SJ, Pinkner JS, et al. Vaccination with FimH adhesin protects cynomolgus monkeys from colonization and infection by uropathogenic Escherichia coli. J Infect Dis. 2000; 181:774–778. [PubMed: 10669375]

Leffler H, Svanborg-Eden C. Chemical identification of a glycosphingolipid receptor for *Escherichia coli* attaching to human urinary tract epithelial cells and agglutinating human erythrocytes. FEMS Microbiol Lett. 1980; 8:127–134.

Lillington J, Geibel S, Waksman G. Biogenesis and adhesion of type 1 and P pili. Biochimica et biophysica acta. 2014; 1840:2783–2793. [PubMed: 24797039]

Loris R, Casset F, Bouckaert J, Pletinckx J, Dao-Thi MH, Poortmans F, Imberty A, Perez S, Wyns L. The monosaccharide binding site of lentil lectin: an X-ray and molecular modelling study. Glycoconjugate journal. 1994; 11:507–517. [PubMed: 7696853]

Miao Y, Li G, Zhang X, Xu H, Abraham SN. A TRP Channel Senses Lysosome Neutralization by Pathogens to Trigger Their Expulsion. Cell. 2015; 161:1306–1319. [PubMed: 26027738]

Mulvey MA, Lopez-Boado YS, Wilson CL, Roth R, Parks WC, Heuser J, Hultgren SJ. Induction and evasion of host defenses by type 1-piliated uropathogenic Escherichia coli. Science. 1998; 282:1494–1497. [PubMed: 9822381]

Mulvey MA, Schilling JD, Hultgren SJ. Establishment of a persistent Escherichia coli reservoir during the acute phase of a bladder infection. Infection and immunity. 2001; 69:4572–4579. [PubMed: 11402001]

Nakagawa T, Kitami Y, Watanabe K, Hanai T, Usuda N, Ogawa A. Increase in lectin binding sites on epithelial cells by chronic bladder infection in rats. Urologia internationalis. 1996; 56:90–95. [PubMed: 8659017]

Nuccio SP, Baumler AJ. Evolution of the chaperone/usher assembly pathway: fimbrial classification goes Greek. Microbiol Mol Biol Rev. 2007; 71:551–575. [PubMed: 18063717]

O'Brien VP, Hannan TJ, Schaeffer AJ, Hultgren SJ. Are you experienced? Understanding bladder innate immunity in the context of recurrent urinary tract infection. Curr Opin Infect Dis. 2015; 28:97–105. [PubMed: 25517222]

Ozer A, Altuntas CZ, Izgi K, Bicer F, Hultgren SJ, Liu G, Daneshgari F. Advanced glycation end products facilitate bacterial adherence in urinary tract infection in diabetic mice. Pathogens and disease. 2015:73.

Pak J, Pu Y, Zhang ZT, Hasty DL, Wu XR. Tamm-Horsfall protein binds to type 1 fimbriated Escherichia coli and prevents E. coli from binding to uroplakin Ia and Ib receptors. The Journal of biological chemistry. 2001; 276:9924–9930. [PubMed: 11134021]

Robino L, Scavone P, Araujo L, Algorta G, Zunino P, Vignoli R. Detection of intracellular bacterial communities in a child with Escherichia coli recurrent urinary tract infections. Pathog Dis. 2013; 68:78–81. [PubMed: 23733378]

Rosen DA, Hooton TM, Stamm WE, Humphrey PA, Hultgren SJ. Detection of intracellular bacterial communities in human urinary tract infection. PLoS Med. 2007; 4:e329. [PubMed: 18092884]

Sanchez JF, Lescar J, Chazalet V, Audfray A, Gagnon J, Alvarez R, Breton C, Imberty A, Mitchell EP. Biochemical and structural analysis of Helix pomatia agglutinin. A hexameric lectin with a novel fold. The Journal of biological chemistry. 2006; 281:20171–20180. [PubMed: 16704980]

Saukkonen KM, Nowicki B, Leinonen M. Role of type 1 and S fimbriae in the pathogenesis of Escherichia coli O18:K1 bacteremia and meningitis in the infant rat. Infection and immunity. 1988; 56:892–897. [PubMed: 2894363]

Schlager TA, LeGallo R, Innes D, Hendley JO, Peters CA. B cell infiltration and lymphonodular hyperplasia in bladder submucosa of patients with persistent bacteriuria and recurrent urinary tract infections. J Urol. 2011; 186:2359–2364. [PubMed: 22019034]

Schwartz DJ, Chen SL, Hultgren SJ, Seed PC. Population Dynamics and Niche Distribution of Uropathogenic Escherichia coli during Acute and Chronic Urinary Tract Infection. Infect Immun. 2011; 79:4250–4259. [PubMed: 21807904]

Schwartz DJ, Conover MS, Hannan TJ, Hultgren SJ. Uropathogenic Escherichia coli Superinfection Enhances the Severity of Mouse Bladder Infection. PLoS Pathog. 2015; 11:e1004599. [PubMed: 25569799]

Stamm WE. Scientific and clinical challenges in the management of urinary tract infections. Am J Med. 2002; 113(Suppl 1A):1S–4S.

Stamm WE, McKevitt M, Roberts PL, White NJ. Natural history of recurrent urinary tract infections in women. Rev Infect Dis. 1991; 13:77–84. [PubMed: 2017637]

Subashchandrabose S, Hazen TH, Brumbaugh AR, Himpsl SD, Smith SN, Ernst RD, Rasko DA, Mobley HL. Host-specific induction of Escherichia coli fitness genes during human urinary tract infection. Proceedings of the National Academy of Sciences of the United States of America. 2014; 111:18327–18332. [PubMed: 25489107]

Tamm I, Horsfall FL. Characterization and Separation of an Inhibitor of Viral Hemagglutination Present in Urine. P Soc Exp Biol Med. 1950; 74:108–114.

Tsuji T, Osawa T. Carbohydrate Structures of Bovine Submaxillary Mucin. Carbohydrate research. 1986; 151:391–402. [PubMed: 3768900]

Wagenlehner FM, Pilatz A, Weidner W, Naber KG. Urosepsis: Overview of the Diagnostic and Treatment Challenges. Microbiology spectrum. 2015:3.

Welch RA, Burland V, Plunkett G 3rd, Redford P, Roesch P, Rasko D, Buckles EL, Liou SR, Boutin A, Hackett J, et al. Extensive mosaic structure revealed by the complete genome sequence of uropathogenic Escherichia coli. Proceedings of the National Academy of Sciences of the United States of America. 2002a; 99:17020–17024. [PubMed: 12471157]

Welch RA, Burland V, Plunkett G, Redford P, Roesch P, Rasko D, Buckles EL, Liou SR, Boutin A, Hackett J, et al. Extensive mosaic structure revealed by the complete genome sequence of uropathogenic Escherichia coli. Proceedings of the National Academy of Sciences of the United States of America. 2002b; 99:17020–17024. [PubMed: 12471157]

Wellens A, Garofalo C, Nguyen H, Van Gerven N, Slattegard R, Hernalsteens JP, Wyns L, Oscarson S, De Greve H, Hultgren S, et al. Intervening with urinary tract infections using anti-adhesives based on the crystal structure of the FimH-oligomannose-3 complex. PloS one. 2008; 3:e2040. [PubMed: 18446213]

Wu XR, Sun TT, Medina JJ. In vitro binding of type 1-fimbriated Escherichia coli to uroplakins Ia and Ib: relation to urinary tract infections. Proceedings of the National Academy of Sciences of the United States of America. 1996; 93:9630–9635. [PubMed: 8790381]

Wurpel DJ, Beatson SA, Totsika M, Petty NK, Schembri MA. Chaperone-usher fimbriae of Escherichia coli. PloS one. 2013; 8:e52835. [PubMed: 23382825]

Wurpel DJ, Totsika M, Allsopp LP, Hartley-Tassell LE, Day CJ, Peters KM, Sarkar S, Ulett GC, Yang J, Tiralongo J, et al. F9 fimbriae of uropathogenic Escherichia coli are expressed at low temperature and recognise Galbeta1-3GlcNAc-containing glycans. PloS one. 2014; 9:e93177. [PubMed: 24671091]

HIGHLIGHTS

- F9/Yde/Fml pili enhance UPEC colonization during chronic urinary tract infection (UTI)
- F9 pilus adhesin FmlH specifically binds Gal(β1-3)GalNac epitopes
- FmlH is upregulated and its receptor is induced during chronic UPEC infection
- Vaccination with FmlH protects against UTI progression

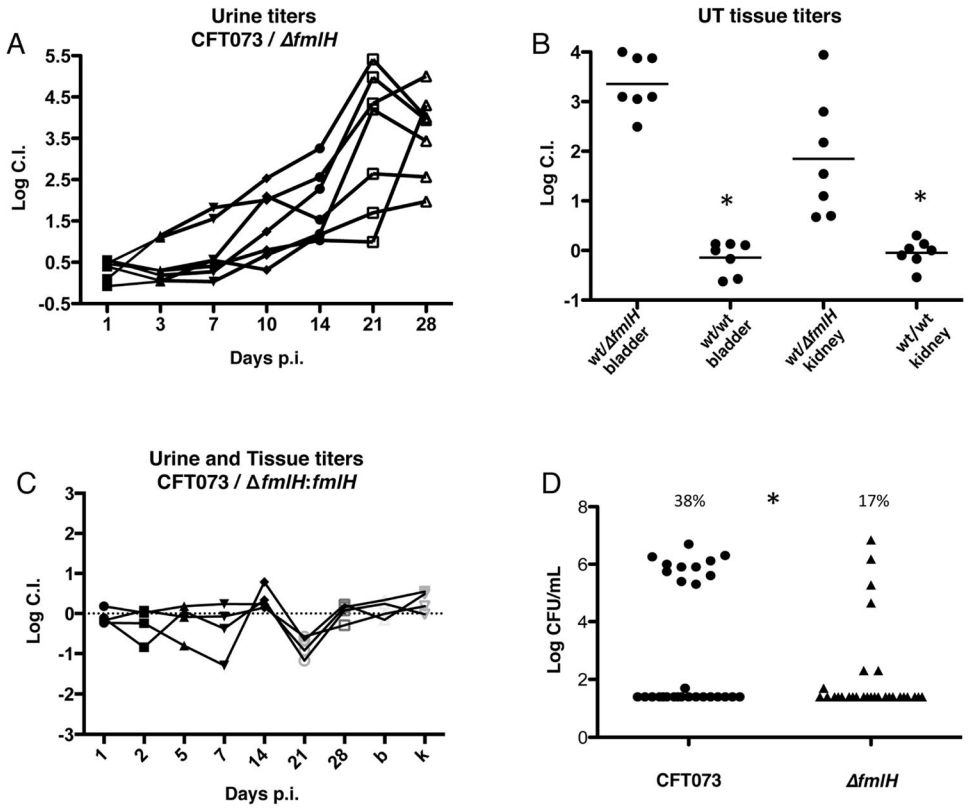

Figure 1. FmlH enhances UPEC colonization during chronic cystitis

(A) The log competitive infection urine titers of C3H/HeN mice infected with equal numbers of CFT073 or CFT073*ΔfmlH* over 28 days. 20 mice were infected over the course of 2 experiments, 7 developed chronic cystitis. (B) Tissue log competitive indexes of mice chronically infected with CFT073 vs. CFT073*ΔfmlH* or CFT073 vs. CFT073 as controls 28 dpi. Asterisk denotes $p<0.05$, Mann-Whitney test. (C) Complementation of *fmlH* restores virulence during chronic cystitis, 10 mice infected and 4 developed chronic cystitis. B and K represent the bladder and kidney titers 28dpi, respectively. (D) Rates of chronic cystitis development in C3H/HeN mice infected with CFT073 (11/29) or *ΔfmlH* (4/29) as represented by bladder bacterial burden 28dpi. Asterisk denotes $p<0.05$, Fisher's exact test. Bars represent the mean of each data set.

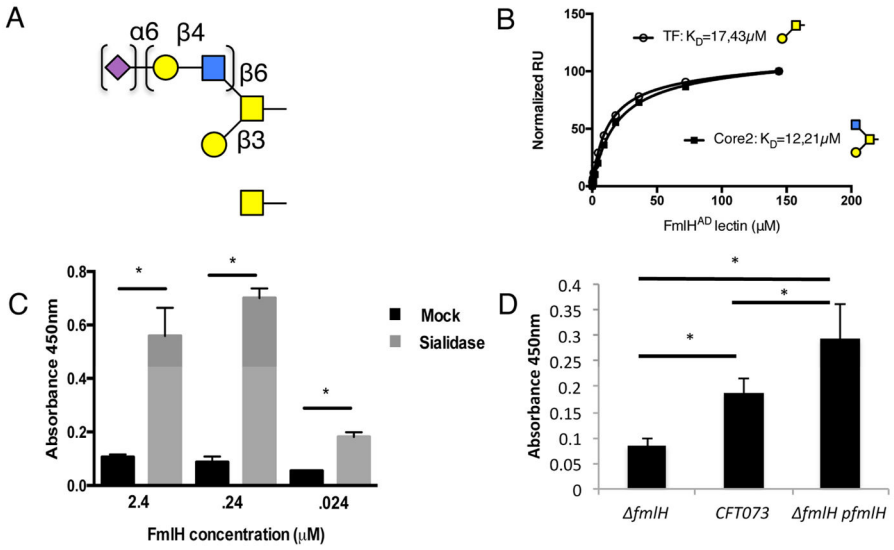

Figure 2. FmlH^{AD} binding to O-glycans

(A) Schematic representation of top-scoring glycan profiles for FmlH^{AD}. Gal, GalNAc, GlcNAc and Neu5Ac are shown as yellow circle and yellow, blue or magenta square, respectively. (B) SPR saturation binding experiments of FmlH^{AD} interacting with immobilized Thomsen-Friedenreich (TF) and Core2 carbohydrates, revealing dissociation constants (K_D) of 17.43 μM and 12.21 μM, respectively. (C) ELISA showing FmlH^{AD} binding to BSM with and without sialidase pretreatment, n=4. (D) ELISA results examining CFT073, CFT073*ΔfmlH*, or CFT073*ΔfmlH:fmlH* binding to sialidase treated BSM coated plates, n=4. Columns represent the mean of each data set and error bars display the standard deviation. Asterisks denote (C) $p<0.0005$ (D) $p<0.05$, Student's t test.

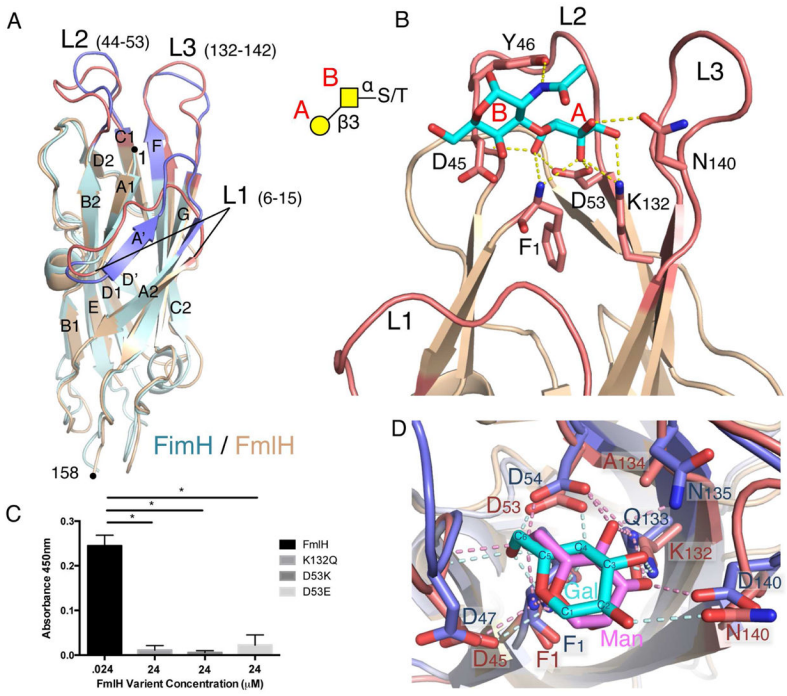

Figure 3. FmlH^{AD}-TF structure and binding specificity

(A) Superimposition of ribbon representation of FmlH^{AD} (tan) and FimH (PDB 2VCO; light blue) lectin domains. The binding pocket regions of FmlH^{AD} (red) and FimH (blue) are formed by loops L1, L2 and L3. (B) Close-up view of the binding pocket region (L1, L2 and L3) of FmlH^{AD} bound to Thomsen-Friedenreich (TF) carbohydrate (Galβ1-3GalNAc; cyan; Gal and GalNAc are labeled A and B, respectively). H bonds are depicted in yellow dashed lines. Inset, schematic representation of the Ser/Thr-Galβ1-3GalNAc motif (TF). (C) Selected point mutants in the FmlH^{AD} binding pocket abolish FmlH^{AD} binding to sialidase treated BSM. (D) Close-up view of FmlH^{AD} (red) and FimH (blue), bound to TF or oligo-mannose 3, respectively (only the reducing end Gal (cyan) or Man (magenta) are shown for comparison). H bonds are depicted in pink (for Gal/FmlH^{AD}) or light blue (for Man/FimH) dashed lines.

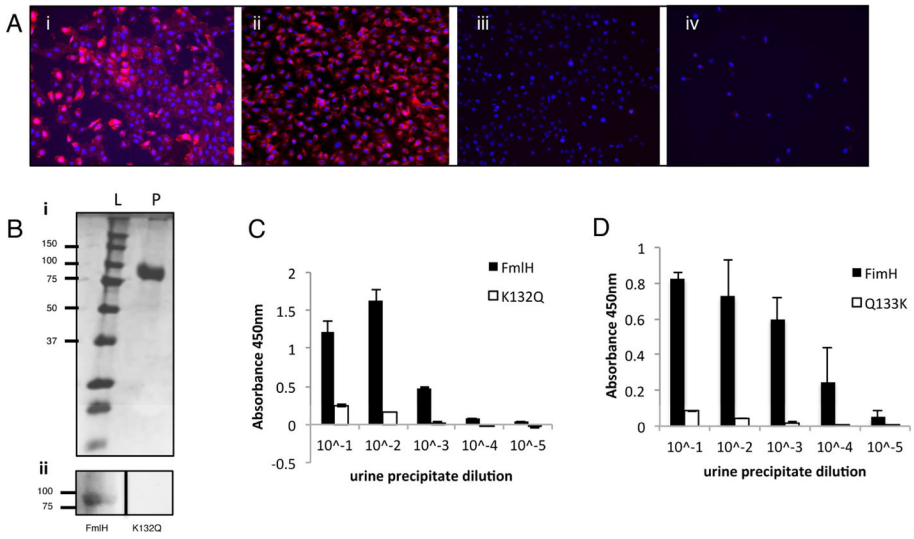

Figure 4. Human uromodulin binding and cell line adherence

(A) FmlH^{AD} binding to human urothelial cell lines. FmlH^{AD} (i and ii) or K132Q (iii and iv) binding (red) to 5637 (i and iii) or T24 (ii and iv) urothelial cell lines. Hoechst DNA staining is represented by the blue in all panels. (B) FmlH^{AD} far western on urine precipitations. Upper panel (i) represents the SDS-PAGE of precipitated urine where L represents the ladder and P the urine protein concentrate. The lower panel (ii) is a Far Western Blot performed on the samples from (i) with FmlH^{AD} or K132Q mutant. (C–D) ELISA showing FmlH^{AD} and FimH binding to urine precipitate. (C) FmlH^{AD} and K132Q or (D) FimH and Q133K binding to human urine protein precipitates. Columns represent the mean of each data set and bars represent the standard deviation.

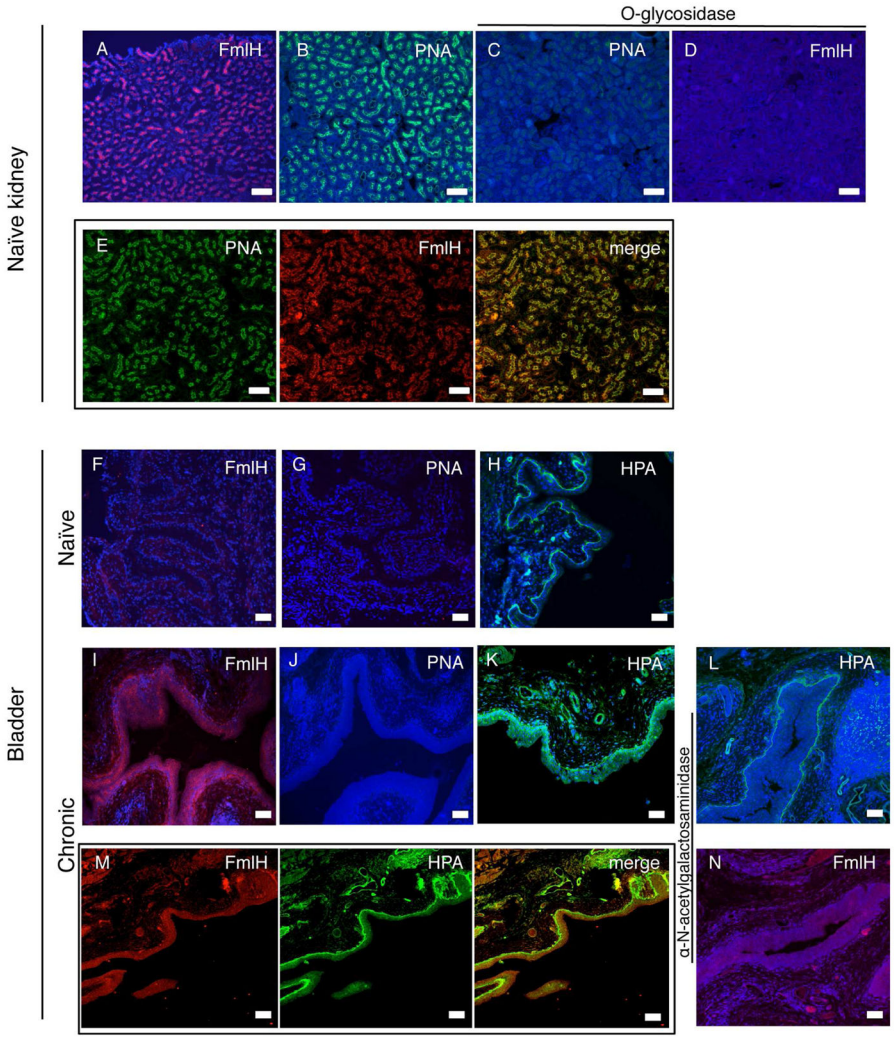

Figure 5. FmlH binding and FmlH receptor analysis in mouse kidney and bladder

Kidney: $FmlH^{ADmC}$ (red) binding to (A) naive kidney tissue. (B) PNA (green) staining of naive kidney tissue. O-glycosidase treatment of naive kidney tissues followed by staining with (C) PNA or (D) $FmlH^{ADmC}$. Co-staining of naïve kidney tissue with (E) PNA (green) and $FmlH^{ADmC}$ (red), merge. Hoechst DNA staining is represented by the blue in all panels. Bladder: $FmlH^{ADmC}$ (red) binding to (F) naïve and (I) chronically infected bladder. PNA staining (green) to (G) naive and (J) chronically infected bladders. HPA staining (green) of (H) naive and (K) chronically infected bladders. Alpha-N-acetylgalactosaminidase treatment of chronically infected bladders followed by (L) HPA or (N) $FmlH^{ADmC}$ staining. Co-staining of chronically infected bladders with (M) HPA (green) and $FmlH^{ADmC}$, merge. Hoechst DNA staining is represented by the blue in all panels. Bar=50μm.

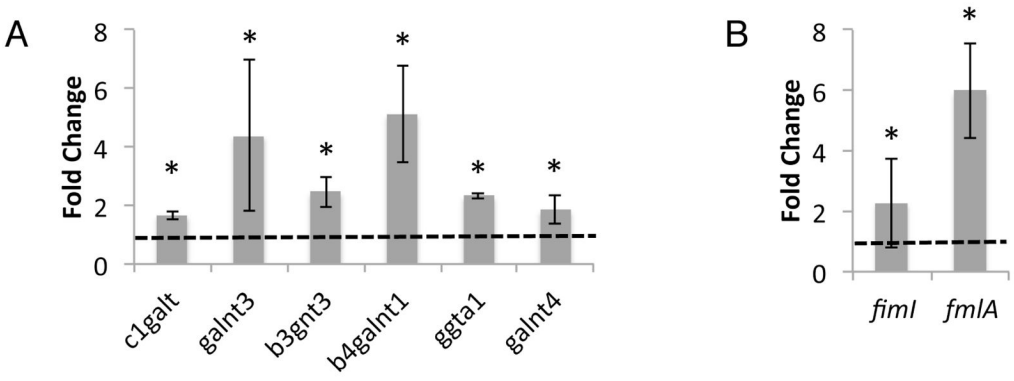

Figure 6. FmlH and FmlH receptor expression during UTI

(A) qPCR of transcripts of selected Gal/GalNAc glycosylhydrolases, shown as fold change in chronically infected versus naïve bladders. **(B)** Measure of type 1 and F9 expression during chronic cystitis by qPCR of the representative pilus subunits *fimI* and *fmlA,* shown as fold change tissue associated versus the inoculum. Columns represent the mean and bars display standard deviation, n=5. Dotted line represents the (A) mock infected or (B) inoculum values. Asterisk denotes $p<0.05$ Wilcoxon Signed Rank test.

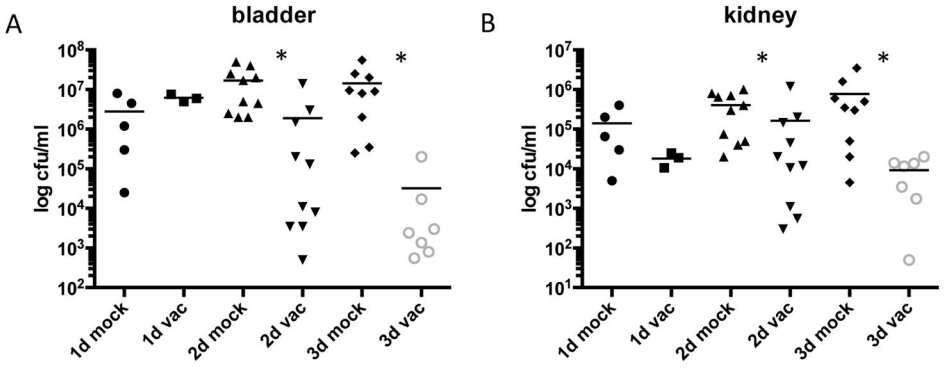

Figure 7. Vaccination with FmlH^{AD} protects against UPEC challenge

C3H/HeN mice were either mock vaccinated or immunized with 30μg of FmlH^{AD}. Mice were subsequently challenged with CFT073 and sacrificed 1, 2 or 3 dpi. Bacterial titers for the (A) bladder and (B) kidney are shown, the bars representing the mean of each sample. Asterisks denote $p<0.05$ Mann-Whitney test.